

# COMPUTATIONAL OPTIMIZATION OF MRTD HAAR-BASED ADAPTIVE SCHEMES USED FOR THE DESIGN OF RF PACKAGING STRUCTURES

Manos M. Tentzeris

School of ECE, Georgia Institute of Technology, Atlanta, GA 30250-0250

(FAX : (404) 894-4641)

(e-mail:etentze@ece.gatech.edu)

## Abstract

The MRTD adaptive gridding scheme that is based on the Haar expansion basis is discussed for arbitrary wavelet resolutions. Guidelines for the optimization of memory and execution time requirements are presented. A multi-time-stepping procedure enhances further the computational economies offered by a combination of absolute and relative thresholding of the wavelet values.

**Keywords: Multiresolution, Time-Domain Techniques, Adaptive Gridding, Wavelets, Memory Compression, Thresholding, Haar**

## I Introduction - Discussion on the Haar expansion basis

Significant attention is being devoted now-a-days to the analysis and design of various types of RF Packaging structures (e.g. Flip-Chip, Multi-Layered Structures) used in Wireless and Computing applications. Though The finite-difference-time-domain (FDTD) scheme is one of the most powerful and versatile techniques used for numerical simulations, it suffers from serious limitations due to the substantial computer resources required to model such electromagnetic problems with medium or large computational volumes. Recently, MRTD (MultiResolution Time Domain Method) [1]–[9] has shown unparalleled properties in comparison to Yee's FDTD. In a MRTD scheme the fields are represented by a two-fold expansion in scaling and wavelet functions with respect to time/space. Scaling functions guarantee a correct modelling of smoothly-varying fields. In regions characterized by strong field variations or field singularities, higher resolution is enhanced by incorporating multiple resolutions of wavelets in the field expansions. The major advantage of the use of Multiresolution analysis to time domain is the capability to develop time and space adaptive grids. This is due to the property of the wavelet expansion functions to interact weakly and allow for a spatial sparsity that may vary with time through a thresholding process. Haar expansion basis functions (Fig.(1)) provide a convenient tool for the transition from FDTD to MRTD due to their compact support, and to their similarity with the FDTD pulse basis [6]–[9]. Nevertheless, the enhancement of additional wavelet terms the number of which is different from cell to cell and for different time-steps requires a careful consideration of the memory and execution time overheads. In addition, the fact that the stability

limit of the time-step decreases as more resolutions are added requires the use of an effective multi-time-stepping algorithm, that will maintain the required accuracy without increasing significantly the execution time requirements.

## II MRTD Scheme with Multiple Wavelet Resolutions

For simplicity, the 1D MRTD scheme for TEM propagation will be discussed. It can be extended to 2D and 3D in a straightforward way. The Electric ( $E_x$ ) and the Magnetic ( $H_y$ ) fields are displaced by half step in both time- and space-domains (Yee cell formulation) and are expanded in a summation of scaling ( $\phi$ ) and wavelet ( $\psi_r$ ) functions in space and scaling components in time. For example,  $E_x$  is given by

$$E_x(z, t) = \sum_{m,i=-\infty}^{\infty} ({}_m E_{x,i}^{\phi} \phi_i(z) + \sum_{r=0}^{r_{max}} \sum_{i_r=1}^{2^r} {}_m E_{x,i}^{\psi_r, i_r} \psi_i^{r, i_r}(z)) \phi_m(t) \quad , \quad (1)$$

where  $\phi_i(z) = \phi(z/\Delta z - i)$  and  $\psi_i^{r, i_r}(z) = 2^{r/2} \psi_0(2^r(z/\Delta z - i_r) - i)$  represent the Haar scaling and  $r$ -resolution wavelet functions located inside the  $i$ -cell. The conventional notation  ${}_m E_{x,i}$  is used for the voltage component at time  $t = m\Delta t$  and  $z = i\Delta z$ , where  $\Delta t$  and  $\Delta z$  are the time-step and the spatial cell size respectively. The notation for  $H_y$  is similar.

Substituting  $E_x, H_y$  in the TEM equations and applying Galerkin technique derives the following equations for  $H_y$

$$\begin{aligned} m+0.5 H_{y,i-0.5}^{\phi} &= m-0.5 H_{y,i-0.5}^{\phi} - \frac{\Delta t}{\mu \Delta z} (E_{x,i}^{\phi} - E_{x,i-1}^{\phi} + \\ &+ \sum_{r=1}^{r_{max}} (c_{1,r,2^r,-1} E_{x,i-1}^{\psi_r, 2^r} + c_{1,r,1,1} E_{x,i+1}^{\psi_r, 1} + \sum_{i_r=1}^{2^r} c_{1,r,i_r,0} E_{x,i}^{\psi_r, i_r}), \end{aligned} \quad (2)$$

$$\begin{aligned} m+0.5 H_{y,i-0.5}^{\psi_0} &= m-0.5 H_{y,i-0.5}^{\psi_0} - \frac{\Delta t}{\mu \Delta z} (E_{x,i}^{\psi_0} - E_{x,i-1}^{\psi_0} + \\ &+ \sum_{r=1}^{r_{max}} (c_{2,r,2^r,-1} E_{x,i-1}^{\psi_r, 2^r} + c_{2,r,1,1} E_{x,i+1}^{\psi_r, 1} + \sum_{i_r=1}^{2^r} c_{2,r,i_r,0} E_{x,i}^{\psi_r, i_r}), \end{aligned} \quad (3)$$

$$\begin{aligned} m+0.5 H_{y,i-0.5}^{\psi_{r'} > 0, i_{r'} \in [1, 2^{r'}-1]} &= m-0.5 H_{y,i-0.5}^{\psi_{r'}, i_{r'}} - \frac{\Delta t}{\mu \Delta z} (d_{r', i_{r'}, 1, -1} E_{x,i-1}^{\phi} + d_{r', i_{r'}, 2, -1} E_{x,i-1}^{\psi_0} \\ &+ \sum_{r=1}^{r_{max}} (\delta_{i_{r'}, 1} e_{r', i_{r'}, r, 2^r, -1} E_{x,i-1}^{\psi_r, 2^r} + \sum_{i_r=i_1}^{i_2} e_{r', i_{r'}, r, i_r, 0} E_{x,i}^{\psi_r, i_r}) \\ &+ \delta_{i_{r'}, 2^{r'}-1} (d_{r', i_{r'}, 1, 0} E_{x,i}^{\phi} + d_{r', i_{r'}, 2, 0} E_{x,i}^{\psi_0}), \end{aligned} \quad (4)$$

$$\begin{aligned} m+0.5 H_{y,i-0.5}^{\psi_{r'} > 0, i_{r'} \in [2^{r'}-1+1, 2^{r'}]} &= m-0.5 H_{y,i-0.5}^{\psi_{r'}, i_{r'}} - \frac{\Delta t}{\mu \Delta z} (d_{r', i_{r'}, 1, 0} E_{x,i}^{\phi} + d_{r', i_{r'}, 2, 0} E_{x,i}^{\psi_0} \\ &+ \sum_{r=1}^{r_{max}} (\delta_{i_{r'}, 2^{i_{r'}}} e_{r', i_{r'}, r, 1, 1} E_{x,i+1}^{\psi_r, 1} + \sum_{i_r=i_1}^{i_2} e_{r', i_{r'}, r, i_r, 0} E_{x,i}^{\psi_r, i_r}) \\ &+ \delta_{i_{r'}, 2^{r'}-1+1} (d_{r', i_{r'}, 1, -1} E_{x,i-1}^{\phi} + d_{r', i_{r'}, 2, -1} E_{x,i-1}^{\psi_0})) \end{aligned} \quad (5)$$

where:  $i_1 = \max[1, \text{INT}((i_r - 1)2^{-(r'-r)} + 1)]$  and  $i_2 = \min[2^r, \text{INT}(1 + i_r 2^{-(r'-r)})]$ . Also, the  $c, d$  and  $e$  coefficients can be calculated by the Galerkin technique correlating the respective wavelet and scaling functions and  $\delta$  is the Kroenecker Delta. For example,

$$c_{1,r,i_r,p} = \int \phi_{i-0.5}(z) \frac{\partial \psi_{i+p}^{r,i_r}(z)}{\partial z} dz = 2^{r/2-1} (\delta_{i_r,2^r} (\delta_{p,-1} - \delta_{p,0}) + \delta_{i_r,1} (\delta_{p,1} - \delta_{p,0})) \quad (6)$$

Through the split of the wavelet coefficients of resolution  $r' > 0$  to two groups ( $[1, \dots, 2^{r'-1}]$  and  $[2^{r'-1} + 1, \dots, 2^{r'}]$ ) the calculations are performed more efficiently in terms of the scaling and wavelet of 0-Resolution contributions. In addition, it is clear that the calculation of these wavelet coefficients require a significantly smaller number of terms than  $2^{r_{max}+1}$ , something that proves that the number of operations increase significantly slower than  $O(2^{2(r_{max}+1)})$  as the maximum resolution  $r_{max}$  increases.

## II.1 Hard Boundaries

Due to the finite-domain nature of the expansion basis, the Hard Boundary conditions (Perfect Electric/Magnetic Conductor) can be easily modeled. For example, if a P.E.C. exists at the  $z = i\Delta z$ , then the scaling  $E_x$  coefficient for the  $i$  - cell has to be set to zero for each time-step  $m$  since the position of the conductor coincides with the midpoint of the domain of the scaling function. Nevertheless, the 0-resolution wavelet for the same cell has the value of zero at its midpoint; thus its amplitude does not have to be set to zero. To enforce the physical condition that the electric field values on either side of the conductor are independent from the fields on the other side, TWO 0-resolution wavelet  $E_x$  coefficients have to be defined. The one (on the one side of P.E.C.) will depend on  $H_y$  values on this side only and the other (on the other side of P.E.C.) will depend on  $H_y$  values on that side only. Wavelet coefficients of higher-resolution with domains tangential to the position of P.E.C. have to be zeroed out as well. As far as it concerns the equations that update the coefficients of the magnetic field  $H_y$ , only  $E_x$  coefficients on the same side of the P.E.C. have to be used. The rest of the summation terms have to be replaced with coefficients derived applying the odd image theory for the electric field. A similar approach can be applied for the modeling of a Perfect Magnetic Conductor (P.M.C.).

It can be easily observed that for Wavelet Resolutions up to  $r_{max}$ ,  $2^{r_{max}+1}$  coefficients have to be calculated per cell per field component instead of one component in the conventional F.D.T.D. The derived gain is that the new algorithm has an improved resolution by a factor of  $2^{r_{max}+1}$  that can vary from cell-to-cell depending on the field variations and discontinuities. In addition, MRTD can offer a significantly better  $E_x$  field resolution close to P.E.C.'s through the 0-Resolution Wavelet Double term with a negligible computational overhead per P.E.C. (the second 0-Resolution term). Conventional F.D.T.D. assumes a constant zero  $E_x$  distribution half-cell on either side of the P.E.C. by zeroing out its amplitude at the P.E.C. cell.

## II.2 Field Reconstruction

The alternating nature of the wavelet functions guarantees the improved time-domain resolution of the MRTD scheme. Assuming that the  $H_y$  scaling and wavelet (0 to  $r_{max}$  resolutions) coefficients for a specific cell  $i$  have been calculated for  $t = m\Delta t$ , two values can be defined for the domain  $[(i - 1. + (i_r - 1)2^{-r_{max}})\Delta z, (i + i_r 2^{-r_{max}})\Delta z]$  of each wavelet coefficient  $\psi_i^{r_{max}, i_r}$  of the maximum resolution  $r_{max}$ . As a result, a total number of  $2^{r_{max}+1}$  subpoints/cell at the positions:  $z = (i - 1. + (i_r - 0.5) 2^{-(r_{max}+1)})\Delta z$ , for  $i_r = 1, \dots, 2^{r_{max}+1}$  can be used for the total field value reconstruction:

$$m_{-0.5} H_y^{total(i, r_{max}, i_r)} = m_{-0.5} H_{y,i}^\phi + c_1 m_{-0.5} H_{y,i}^{\psi_0} + \sum_{r=1}^{r_{max}} m_{-0.5} H_{y,i}^{\psi_{r,i_r}} \psi_{r,i_r}(z) \quad , \quad (7)$$

where:  $i_r' = INT(2^r z) + 1$ , and

$$c_1 = \begin{cases} +1 & \text{if } i_r \leq 2^{r_{max}} \\ -1 & \text{if } i_r > 2^{r_{max}} \end{cases}$$

A similar expression can be derived for  $E_x$  component. It is obvious, that only  $2 + r_{max}$  coefficients are required for the field reconstruction at each subpoint.

## II.3 Dynamic Adaptivity - Thresholding

The fact that the wavelet coefficients take significant values only for a small number of cells that are close to abrupt discontinuities or contain fast field variations allows for the development of a dynamically adaptive gridding algorithm. One thresholding technique based on absolute and relative thresholds offers very significant economy in memory while maintaining the increased resolution in space where needed. For each time-step, the values of the scaling coefficients are first calculated for the whole grid. Then, wavelet coefficients with resolutions of increasing order are updated. As soon as all wavelet components of a specific resolution of a cell have values below the Absolute Threshold (that has to do with the numerical accuracy of the algorithm) or below a specific fraction (Relative Threshold) of the respective scaling coefficient, no higher wavelet resolutions are updated and the simulation moves to the update of the wavelet coefficients of the next cell. The same thresholding procedure is performed for both  $E_x$  and  $H_y$  components. of the respective medium(s). In this way, the execution time requirements are optimized, since for areas away from the excitation or discontinuities, only the scaling coefficients need to be updated. This is a fundamental difference with the conventional F.D.T.D. algorithms that cannot provide a dynamical time- and space- adaptivity even with grids of variable cell sizes (static adaptivity).

## II.4 Multi-Time-Stepping Implementation

As it has been reported in [9], the maximum time step value that guarantees numerical stability for maximum wavelet resolution  $r_{max}$  is

$$\Delta t^{(r_{max})} = \frac{\Delta z}{2^{r_{max}} c} \quad , \quad (8)$$

where  $c$  is the velocity of the light in the simulated medium and  $\Delta t$ ,  $\Delta z$  are the time-step and the cell size respectively. The dynamically changing gridding that was described in the previous section allocates different values of maximum wavelet resolution throughout the grid for every time-step, thus deriving different values of stable time-steps from cell to cell. The easiest way to guarantee stability would be to identify the maximum used wavelet resolution and use the respective time-step. That would lead to a huge computational overhead of no practical gain especially for cells that a few or even no wavelet resolution is needed. On the other side, if different time-steps were to be used, the calculation of coefficients updated more often than the neighboring cells (high wavelet resolutions and smaller time-steps) would require the efficient interpolation of the values that are updated less often (larger time-steps). To simplify this procedure, the used time-steps in the grid are defined in powers of 2 starting from the smallest time-step (cells that use the highest wavelet resolution  $r_{max}$ ),  $\Delta t^{(r_{max})}$ . For example, the used time-step for a cell that requires the wavelet calculation up to the  $r_{use} < r_{max}$  resolution would get the value  $\Delta t^{(r_{use})} = \Delta t^{(r_{max})} 2^{r_{max}-r_{use}}$ .

After identifying the appropriate time-steps for each cell, a second-order backward interpolation is used to calculate field values for intermediate time instants. For example, if the calculation of  $E_x$  coefficients in one cell is performed with time-step  $\delta t = \Delta t^{(r_1)}$  and the calculation of  $H_y$  in the neighboring cell is performed with a larger  $\Delta t = \Delta t^{(r_2)} = \delta t 2^{r_1-r_2}$ , there is the need for the calculation of  $H_y$  in  $2^{r_1-r_2}$  subpoints between  $m\Delta t$  and  $(m+1)\Delta t$  for each time-step  $m$ . The interpolation process can be expressed as:

$$\begin{aligned}
{}_{i_{int}}H_y &= \left[ \left( 0.5 + (i_{int} - 0.5) \frac{\delta t}{\Delta t} \right) \left( 1 + 0.5 \left( (i_{int} - 0.5) \frac{\delta t}{\Delta t} - 0.5 \right) \right) \right] {}_{m+0.5}H_y \\
&- \left[ \left( (i_{int} - 0.5) \frac{\delta t}{\Delta t} - 0.5 \right) \left( 1 + (i_{int} - 0.5) \frac{\delta t}{\Delta t} + 0.5 \right) \right] {}_{m-0.5}H_y \\
&+ 0.5 \left[ (i_{int} - 0.5) \frac{\delta t}{\Delta t} - 0.5 \right] \left[ (i_{int} - 0.5) \frac{\delta t}{\Delta t} + 0.5 \right] {}_{m-1.5}H_y \quad , \quad (9)
\end{aligned}$$

for  $i_{int} = 1, \dots, \frac{\Delta t}{\delta t} (= 2^{r_1-r_2})$  and can be applied to scaling and wavelet components. The use of the second-order scheme provides stability for thousands of time-steps. Using linear time interpolation was found to lead to instabilities and increased reflection error at the interface of the different time-steps. Though the interpolation process adds a computational overhead by requiring the storage of the coefficients for three time-steps, it improves significantly the requirements in execution time by performing the simulations at the maximum allowable time-step everywhere in the grid.

## II.5 Validation Case

To validate the above approach, the MRTD algorithm was applied to the simulation of the TEM propagation of a Gaussian excitation at  $z = 200\Delta z$  up to 3 GHz inside air dielectric ( $\epsilon_r = \mu_r = 1$ ) for 1,000 time-steps with size  $\Delta t = 0.95\Delta t^{r_{max}}$  for each cell's maximum used wavelet resolution  $r_{max}$  and 400 cells with  $\Delta z = 2.5cm$ . Wavelets up to 2-Resolution are enhanced wherever needed. A relative threshold of  $10^{-4}$  and an absolute threshold of  $10^{-6}$  offer an approximation error smaller than 0.4%. Fig.(2) which displays the reconstructed  $E_x$  field distribution at  $t = 500\Delta z$  demonstrates

the fact that only 24 cells need to calculate the Wavelet Coefficients. Everywhere else  $E_x$  is close to zero and shows no variation; thus it requires the calculation of only scaling coefficients. (Memory Compression=94%). The fact that an interpolation scheme is used for the time-stepping allows for a time-step aspect ratio of  $2^3 = 8 : 1$  in these two areas. In this way, the memory compression gain is transferred to the execution time as well without affecting the simulation accuracy. Fig.(3) which is a magnification of Fig.(2) for the area of increased resolution, proves the ability of Haar-based MRTD schemes with arbitrary wavelet resolutions to provide locally magnified accuracy through the accurate representation of field variations at multiple intracell subpoints. This optimized algorithm has been expanded in 2D and 3D and simulation results of practical RF Packaging structures (Flip-Chip, Embedded Passives) will be presented at the conference. intracell subpoints.

### III Conclusions

Various computational aspects concerning the Haar-based MRTD adaptive gridding scheme have been discussed and guidelines for the optimization of memory and execution time requirements have been presented. The use of absolute and relative thresholding of the wavelet coefficients has been combined with a multi-time-stepping procedure and has led to further economies. In addition, an optimized field reconstruction procedure allows for the quick and reliable demonstration of the increased resolution that is offered by the enhancement of multiple resolution of wavelets with minimum computational overhead. In this way, the Haar-based MRTD adaptive scheme has been proven to be a very efficient and reliable full-wave simulation tool for complex RF structures, such as RF Packaging geometries.

### IV Acknowledgments

The author would like to thank the Packaging Research Center of Georgia Tech for their continuous support.

### References

- [1] E.Tentzeris, R.Robertson, A.Cangellaris and L.P.B. Katehi, "Space- and Time- Adaptive Gridding Using MRTD", Proc. MTT-S 1997, pp. 337-340.
- [2] M.Krumpholz, L.P.B.Katehi, "MRTD: New Time Domain Schemes Based on Multiresolution Analysis", IEEE Trans. Microwave Theory and Techniques, vol. 44, no. 4, pp. 555-561, April 1996.
- [3] E.Tentzeris, M.Krumpholz and L.P.B. Katehi, "Application of MRTD to Printed Transmission Lines", Proc. MTT-S 1996, pp. 573-576.
- [4] R. Robertson, E. Tentzeris, M. Krumpholz, L.P.B. Katehi, "Application of MRTD Analysis to Dielectric Cavity Structures", Proc. MTT-S 1996, pp. 1861-1864.
- [5] E.Tentzeris, R.Robertson, M.Krumpholz and L.P.B. Katehi, "Application of the PML Absorber to the MRTD Technique", Proc. AP-S 1996, pp. 634-637.
- [6] E.Tentzeris, J.Harvey and L.P.B.Katehi, "Time Adaptive Time-Domain Techniques for the Design of Microwave Circuits", IEEE Microwave and Guided Wave Letters, Vol. 9, No. 3, pp. 96-98, 1999.
- [7] K.Goverdhanam, E.Tentzeris, M.Krumpholz and L.P.B. Katehi, "An FDTD Multigrid based on Multiresolution Analysis", Proc. AP-S 1996, pp. 352-355.

- [8] M.Fujii, W.J.R.Hoefler, "Formulation of a Haar-wavelet based Multiresolution Analysis similar to the 3-D FDTD Method", Proc. MTT-S 1998, pp. 1393-1396.
- [9] C.Sarris and L.P.B.Katehi, "Multiresolution Time Domain (MRTD) Schemes with Space-Time Haar Wavelets", Proc. MTT-S 1999, pp. 1459-1462

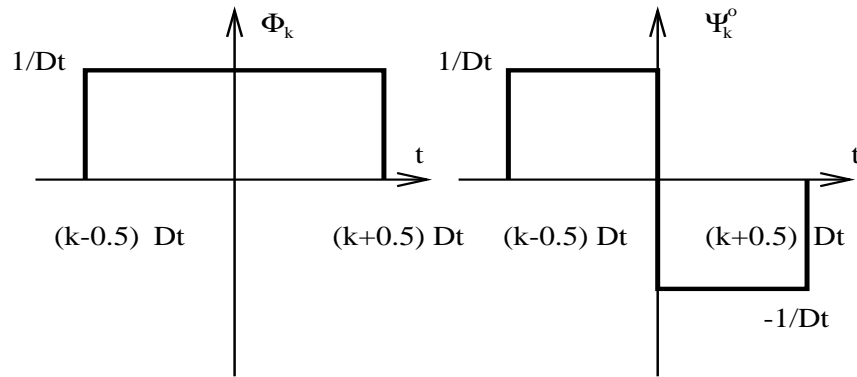


Figure 1: 0-Order Haar Function Basis.

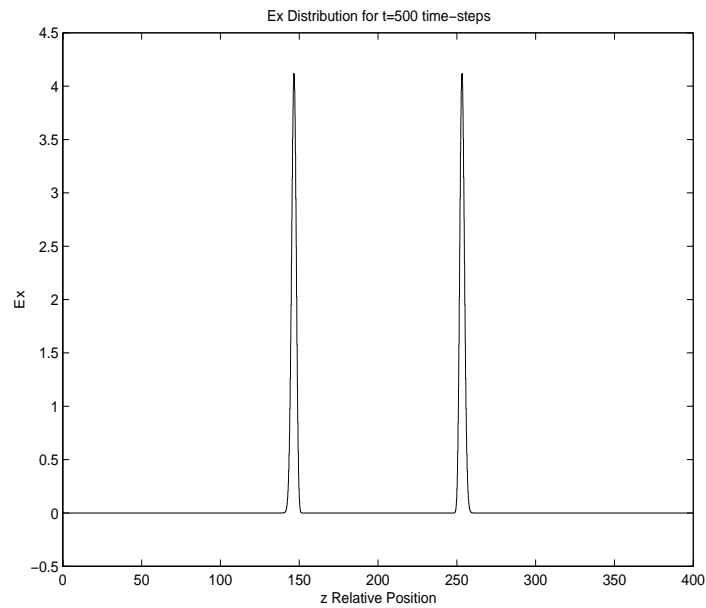
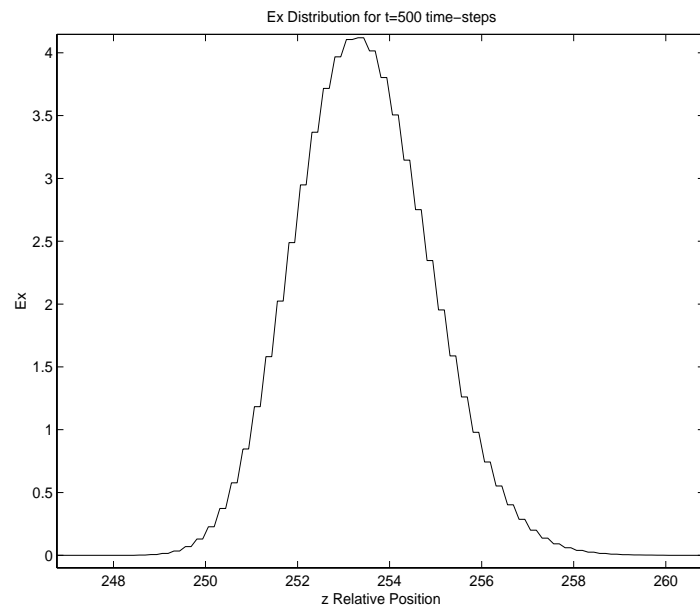


Figure 2: Demonstration of the Memory Compression of  $E_x$  Spatial Distribution at  $t = 500\Delta t$ .



**Figure 3: Demonstration of the Variable Resolution (Multipoint Intracell Representation) of  $E_x$  Spatial Distribution at  $t = 500\Delta t$ .**